nature biotechnology

Fusion of catalytically inactive Cas9 to FokI nuclease improves the specificity of genome modification

John P Guilinger[1–3], David B Thompson[1–3] & David R Liu[1,2]

Genome editing by Cas9, which cleaves double-stranded DNA at a sequence programmed by a short single-guide RNA (sgRNA), can result in off-target DNA modification that may be detrimental in some applications. To improve DNA cleavage specificity, we generated fusions of catalytically inactive Cas9 and FokI nuclease (fCas9). DNA cleavage by fCas9 requires association of two fCas9 monomers that simultaneously bind target sites ~15 or 25 base pairs apart. In human cells, fCas9 modified target DNA sites with >140-fold higher specificity than wild-type Cas9 and with an efficiency similar to that of paired Cas9 'nickases', recently engineered variants that cleave only one DNA strand per monomer. The specificity of fCas9 was at least fourfold higher than that of paired nickases at loci with highly similar off-target sites. Target sites that conform to the substrate requirements of fCas9 occur on average every 34 bp in the human genome, suggesting the versatility of this approach for highly specific genome-wide editing.

The recent development of robust, predictable and user-friendly methods for the generation of sequence-specific, DNA-binding proteins has accelerated the use of genome editing for biological research[1] and therapeutic development[2]. The clustered, regularly interspaced, short palindromic repeats (CRISPR)–associated protein 9 (Cas9) system is an especially convenient approach for genome editing, as an agent for a new target site of interest can be created simply by generating the corresponding sgRNA. The 3′ end of the sgRNA forms a scaffold that binds Cas9 protein[3], whereas the ~17 to 20 bases[4] at the 5′ end of the sgRNA pair with the target DNA to determine DNA cleavage specificity (**Fig. 1**). Provided that the target sequence is adjacent to a short 3′ motif—the protospacer adjacent motif (PAM) required for initial binding and Cas9 activation[5]—any DNA locus can in principle be targeted. In cells, double-strand breaks induced by targeted Cas9:sgRNA complexes enable either functional gene knockout through nonhomologous end joining (NHEJ) or alteration of a target locus to virtually any sequence through homology-directed repair with an exogenous DNA template[3,6,7].

The usefulness of Cas9 for research and therapeutic applications may be limited by its ability to cleave off-target genomic sites[8–12]. We hypothesized that engineering Cas9 variants to cleave DNA only when two simultaneous, adjacent Cas9:DNA binding events take place could substantially improve specificity because the likelihood of two adjacent off-target binding events is much smaller than the likelihood of a single off-target binding event (approximately $1/n^2$ versus $1/n$). This approach is analogous to that previously developed for dimeric zinc-finger nucleases (ZFNs) and TALENs. Based on those examples, we speculated that fusing the FokI restriction endonuclease cleavage domain to a catalytically dead Cas9 (dCas9) could create an obligate dimeric Cas9 that would cleave DNA only when two distinct FokI-dCas9:sgRNA complexes bind to adjacent sites ("half-sites") with particular spacing constraints (**Fig. 1a**).

This approach is distinct from the use of 'nickases', mutant Cas9 proteins that cleave only a single strand of double-stranded (dsDNA). Paired nickases can be used to nick opposite strands of two nearby target sites, generating what is effectively a double-strand break, and can induce substantial on-target DNA modification with reduced off-target modification[4,12–14]. Because each of the component Cas9 nickases remains catalytically active[5,6,15], and single-stranded DNA cleavage events are weakly mutagenic[16,17], nickases can induce genomic modification even when acting as monomers[5,13,18]. Moreover, because paired Cas9 nickases can efficiently induce dsDNA cleavage–derived modification events when bound up to ~100 bp apart[13,14], the statistical number of potential off-target sites for paired nickases is larger than that of a more spatially constrained dimeric Cas9 cleavage system. In contrast, DNA cleavage by FokI-dCas9 requires simultaneous binding of two distinct FokI-dCas9 monomers because monomeric FokI nuclease domains are not catalytically competent[18]. In principle, this approach should increase the specificity of DNA cleavage relative to wild-type Cas9 by doubling the number of specified target bases. The use of fCas9 should also result in improved specificity compared to nickases due to the inactivity of monomeric FokI-dCas9:sgRNA complexes and due to the more stringent spatial requirements for assembly of a FokI-dCas9 dimer.
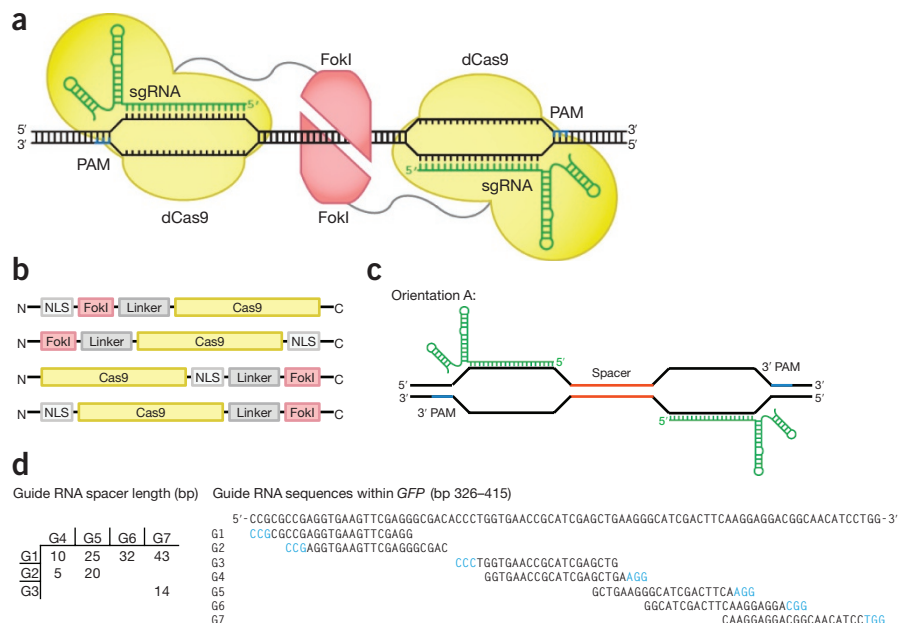
RESULTS
Development of an active FokI-dCas9 fusion architecture
We began by constructing and characterizing a wide variety of FokI-dCas9 fusion proteins with distinct configurations of a FokI nuclease domain, a dCas9 containing inactivating mutations D10A and H840A, and a nuclear localization sequence (NLS). We fused wild-type, homodimeric, FokI to either the N or C terminus of dCas9 and varied the location of the NLS to be at either terminus or between the

[1]Department of Chemistry & Chemical Biology, Harvard University, Cambridge, Massachusetts, USA. [2]Howard Hughes Medical Institute, Harvard University, Cambridge, Massachusetts, USA. [3]These authors contributed equally to this work. Correspondence should be addressed to D.R.L. (drliu@fas.harvard.edu).

Figure 1 Architectures of Cas9 and FokI-dCas9 fusion variants. (**a**) Two monomers of FokI nuclease (red) fused to dCas9 (yellow) bind in complex with guide RNAs (sgRNA, green) to separate sites within the target locus. Only adjacently bound FokI-dCas9 monomers can assemble a catalytically active FokI nuclease dimer, triggering dsDNA cleavage. (**b**) FokI-dCas9 fusion architectures tested. Four distinct configurations of NLS, FokI nuclease and dCas9 were assembled. 17 protein linker variants were also tested. (**c**,**d**) sgRNA orientation (**c**) and target sites tested within *GFP* (**d**). Seven sgRNA target sites were chosen to test FokI-dCas9 activity in an orientation in which the PAM is distal from the cleaved spacer sequence (orientation A). Together, these seven sgRNAs enabled testing of FokI-dCas9 fusion variants across seven spacer lengths ranging from 5 to 43 bp. (See **Supplementary Fig. 1** for guide RNAs used to test orientation B, in which the PAM is adjacent to the spacer sequence.)

two domains (**Fig. 1b** and **Supplementary Notes**). We further varied the length of the linker sequence as either one or three repeats of Gly-Gly-Ser (GGS) between the FokI and dCas9 domains. As previously developed dimeric nuclease systems are sensitive to the length of the spacer sequence between half-sites[19,20], we also tested a wide range of spacer sequence lengths between two sgRNA binding sites within a test target gene, Emerald GFP (Life Technologies) (referred to hereafter as GFP) (**Fig. 1c,d** and **Supplementary Fig. 1**).

We chose two sets of sgRNA binding-site pairs with different orientations within GFP. One set placed the pair of NGG PAM sequences distal from the spacer sequence, with the 5′ end of the sgRNA adjacent to the spacer (orientation A) (**Fig. 1c**), whereas the other placed the PAM sequences immediately adjacent to the spacer (orientation B) (**Supplementary Fig. 1**). In total, seven pairs of sgRNAs were suitable for orientation A and six were suitable for orientation B. By pairwise combination of the sgRNA targets, we tested spacer lengths in both dimer orientations, ranging from 5 to 43 bp in orientation A, and 4 to 42 bp in orientation B. In total, 216 pairs of FokI-dCas9:sgRNA complexes were generated and tested, exploring four fusion architectures, 17 protein linker variants (described below), both sgRNA orientations and 13 spacer lengths between half-sites.

To assay the activities of these candidate FokI-dCas9:sgRNA pairs, we used a previously described flow cytometry–based fluorescence assay[4,9] in which DNA cleavage and NHEJ of a stably integrated constitutively expressed *GFP* gene in HEK293 cells leads to loss of cellular fluorescence (**Supplementary Fig. 2**). For comparison, we assayed the initial set of FokI-dCas9 variants side-by-side with the corresponding Cas9 nickases and wild-type Cas9 in the same expression plasmid across both sgRNA spacer orientation sets A and B. Cas9 protein variants and sgRNA were generated in cells by transient co-transfection of the corresponding Cas9 protein expression plasmids together with the appropriate pair of sgRNA expression plasmids. The FokI-dCas9 variants, nickases and wild-type Cas9 all targeted identical DNA sites using identical sgRNAs. Although this assay showed a consistent ~5% background signal in the absence of sgRNA, it enabled the rapid assessment of many fusion constructs, sgRNA orientations and DNA spacer lengths to identify active constructs for further optimization.

Most of the initial FokI-dCas9 fusion variants were inactive or very weakly active (**Supplementary Fig. 3**). Only the NLS-FokI-dCas9 architecture resulted in a frequency of GFP-negative cells that was substantially higher than what was observed in the corresponding no-sgRNA control when used in orientation A (with PAMs distal from the spacer) (**Supplementary Fig. 3a**). By contrast, NLS-FokI-dCas9 activity above background was not detected when used with sgRNA pairs in orientation B, with PAMs adjacent to the spacer (**Supplementary Fig. 3b**). Examination of the recently reported Cas9 structures[21,22] reveals that the Cas9 N terminus protrudes from the RuvC domain, which contacts the 5′ end of the sgRNA:DNA duplex. We speculate that this arrangement places an N-terminally fused FokI distal from the PAM, resulting in a preference for sgRNA pairs with PAMs distal from the cleaved spacer (**Fig. 1a**). Further, examination of the structure of the C terminus of dCas9 suggests that access to the spacer by FokI C-terminal fusions may require longer linkers to span the PI and RuvC Cas9 domains with paired sgRNAs in orientation A, or to span the REC1 domain of Cas9 and sgRNA stem loops with sgRNAs in orientation B. Although other FokI-dCas9 fusion pairings and the other sgRNA orientation in some cases showed modest activity (**Supplementary Fig. 3**), we chose NLS-FokI-dCas9 with sgRNAs in orientation A for further development.

Optimizing and validating the NLS-FokI-dCas9 architecture

Next we optimized the protein linkers between the NLS and FokI domain and between the FokI domain and dCas9 in the NLS-FokI-dCas9 architecture. We tested 17 linkers with a wide range of amino acid compositions, predicted flexibilities and lengths varying from 9 to 21 residues (**Supplementary Fig. 4a**). For the linker between the FokI domain and dCas9, the highest levels of genomic GFP modification was observed for the proteins with a flexible 18-residue linker $(GGS)_6$ and a 16-residue "XTEN" linker, which was based on a previously reported engineered protein with an open, extended conformation[23] (FokI-L8 in **Supplementary Fig. 4a,b** and **Supplementary Results**). Many of the FokI-dCas9 linkers tested including the optimal XTEN linker resulted in nucleases with a marked preference for spacer lengths of ~15 and ~25 bp between half-sites, with all other spacer lengths, including 20 bp, showing substantially lower activity (**Supplementary Fig. 4b**). This pattern of linker preference is consistent with a model in which the FokI-dCas9

fusions must bind to opposite faces of the DNA double helix to cleave DNA, with optimal binding taking place ~1.5 or 2.5 helical turns apart. The variation of the NLS-FokI linkers did not strongly affect nuclease performance, especially when combined with the XTEN FokI-dCas9 linker (**Supplementary Fig. 4b** and **Supplementary Results**).

The NLS-GGS-FokI-XTEN-dCas9 construct consistently exhibited the highest activity among the tested candidates, inducing loss of GFP in ~10% of cells over background, compared to ~15% and ~25% for Cas9 nickases and wild-type Cas9 nuclease, respectively (**Fig. 2a**). All subsequent experiments were done using this construct, hereafter referred to as fCas9. To confirm the ability of fCas9 to efficiently modify genomic target sites, we used the T7 endonuclease I Surveyor assay to measure the amount of mutation at each of seven target sites within the integrated *GFP* gene in HEK293 cells treated with fCas9, Cas9 nickase or wild-type Cas9, and either of two distinct sgRNAs in orientation A or no sgRNAs as a negative control. Consistent with our flow cytometry–based studies, fCas9 was able to modify the GFP target sites with optimal spacer lengths of ~15 or ~25 bp at a rate of ~20%, comparable to the efficiency of nickase-induced modification and approximately two-thirds that of wild-type Cas9 (**Fig. 2a–c**).

Modification of endogenous genomic targets by optimized fCas9
Next, we evaluated the ability of the optimized fCas9 to modify 14 distinct endogenous genomic loci in five genes by Surveyor assay. *AAVS1* (one site), *CLTA* (two sites), *EMX* (two sites), *HBB* (six sites) and *VEGF* (three sites) were targeted with two sgRNAs per site in orientation A spaced at various lengths (**Supplementary Fig. 5**). Consistent with the results of the experiments targeting GFP, at appropriately spaced target half-sites, fCas9 induced efficient modification of all five genes, with efficiencies ranging from 8% to 22% (**Fig. 2d–h** and **Supplementary Fig. 6**). With the sgRNA spacer lengths resulting in the highest modification at each of the six genes targeted (including GFP), fCas9 induced on average 14.9% (±6.0% s.d.) modification, whereas Cas9 nickase and wild-type Cas9 induced on average 20.6% (±5.6% s.d.) and 28.2% (±6.2% s.d.) modification, respectively. Because decreasing the amount of Cas9 expression plasmid and sgRNA expression plasmid during transfection generally did not proportionally decrease genomic modification activity for Cas9 nickase and fCas9 (**Supplementary Fig. 7a–c**), expression was likely not limiting under the conditions tested.

Stringent spatial requirements of fCas9-mediated DNA cleavage
As the sgRNA requirements of fCas9 potentially reduce the number of potential off-target substrates of fCas9, we compared the effect of guide RNA orientation on the ability of fCas9, Cas9 nickase and wild-type Cas9 to cleave target GFP sequences. Consistent with previous reports[12–14], Cas9 nickase efficiently cleaved targets when guide RNAs
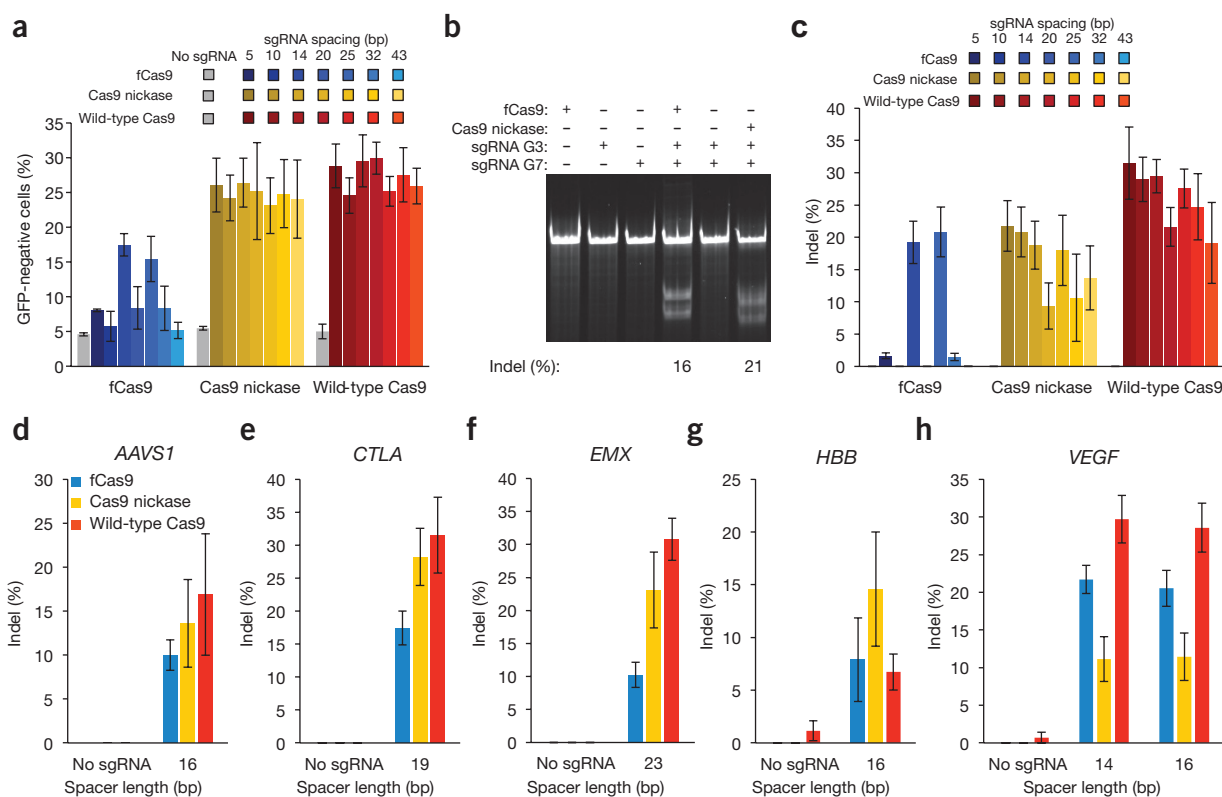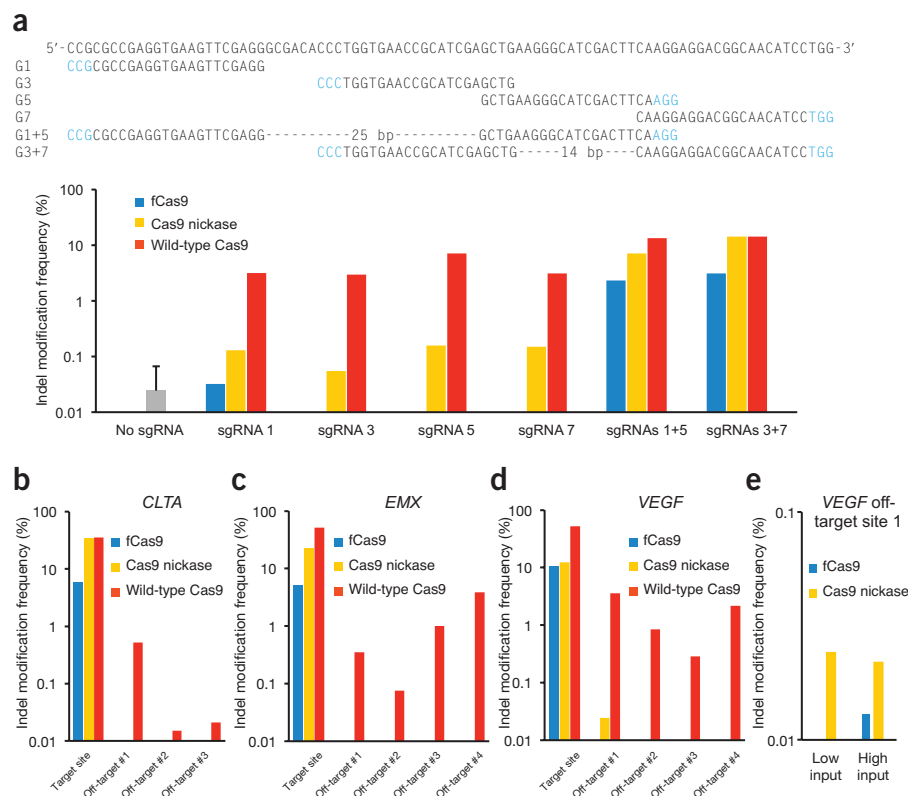

Figure 2 Genomic DNA modification by fCas9, Cas9 nickase and wild-type Cas9. Detection of genomic modification by loss of GFP signal or Surveyor assay at either an integrated *GFP* gene, or at endogenous genomic targets within the *AAVS1*, *CLTA*, *EMX*, *HBB* or *VEGF* genes (**Supplementary Fig. 5**). (**a**) GFP disruption activity of fCas9, Cas9 nickase or wild-type Cas9 with either no sgRNA or sgRNA pairs of variable spacer length targeting the *GFP* gene in orientation A. (**b**) Indel modification efficiency from PAGE analysis of a Surveyor cleavage assay of renatured target-site DNA amplified from cells treated with fCas9, Cas9 nickase or wild-type Cas9 and two sgRNAs spaced 14 bp apart targeting the *GFP* site (sgRNAs G3 and G7; **Fig. 1d**), each sgRNA individually, or no sgRNAs. The indel modification percentage is shown below each lane for samples with modification above the detection limit (~2%). (**c–h**) Indel modification efficiency for two pairs of sgRNAs spaced 14 or 25 bp apart targeting the *GFP* site (**c**), on a pair of sgRNAs spaced 16 bp apart targeting the *AAVS1* site (**d**), one pair of sgRNAs spaced 19 bp apart targeting the *CLTA* site (**e**), one pair of sgRNAs spaced 23 bp apart targeting the *EMX* site (**f**), one pair of sgRNAs spaced 16 bp apart targeting the *HBB* site (**g**) and two pairs of sgRNAs spaced 14 or 16 bp apart targeting the *VEGF* site (**h**). Error bars reflect s.e.m. from three biological replicates performed on different days.

Figure 3 DNA modification specificity of fCas9, Cas9 nickase, and wild-type Cas9. (**a**) Results from high-throughput sequencing of *GFP* on-target sites amplified from 150 ng genomic DNA isolated from human cells treated with a plasmid expressing wild-type Cas9, Cas9 nickase or fCas9; and either a plasmid expressing a single sgRNA (G1, G3, G5 or G7), or two plasmids each expressing a different sgRNA (G1+G5 or G3+G7). As a negative control, transfection and sequencing were done in triplicate as above without any sgRNA expression plasmids. Sequences with more than one insertion or deletion at the GFP target site (the start of the G1 binding site to the end of the G7 binding site) were considered indels. Indel percentages are the number of indels observed, divided by the total number of sequences. Although wild-type Cas9 produced indels across all sgRNA treatments, fCas9 and Cas9 nickase produced indels efficiently (>1%) only when paired sgRNAs were present. Indels induced by fCas9 and single sgRNAs were not detected at a frequency above that of the no-gRNA control, whereas Cas9 nickase and single sgRNAs modified the target GFP sequence at an average rate of 0.12%. (**b**–**e**) The indel mutation frequency from high-throughput DNA sequencing of amplified genomic on-target sites and off-target sites from cells treated with fCas9, Cas9 nickase or wild-type Cas9 and two sgRNAs spaced 19 bp apart targeting the *CLTA* site (sgRNAs C1 and C2) (**b**),

two sgRNAs spaced 23 bp apart targeting the *EMX* site (sgRNAs E1 and E2) (**c**), or two sgRNAs spaced 14 bp apart targeting the *VEGF* site (sgRNAs V1 and V2) (**d**,**e**). (**e**) Two in-depth trials to measure genome modification at *VEGF* off-target site 1. The low-input trial used 150 ng of genomic input DNA and $>8 \times 10^5$ sequence reads for each sample; the high-input trial used 600 ng of genomic input DNA and $>23 \times 10^5$ sequence reads for each sample. In **b**–**e**, all significant ($P < 0.005$ Fisher's exact test) indel frequencies are shown. P values are listed in **Supplementary Table 3**. For **b**–**e** each on- and off-target sample was sequenced once with >10,000 sequences analyzed per on-target sample and an average of 76,260 sequences analyzed per off-target sample (**Supplementary Table 3**).

were bound either in orientation A or orientation B, similar to wild-type Cas9 (**Supplementary Fig. 8a,b**). In contrast, fCas9 only cleaved the GFP target when guide RNAs were aligned in orientation A (**Fig. 2a–c** and **Supplementary Fig. 8a,b**). This orientation requirement further limits opportunities for undesired off-target DNA cleavage.

No modification was observed by GFP disruption or Surveyor assay when any of four single sgRNAs were expressed individually with fCas9, as expected because two simultaneous binding events are required for FokI activity (**Fig. 2b** and **Supplementary Fig. 9**). By contrast, *GFP* gene disruption resulted from expression of any single sgRNA with wild-type Cas9 (as expected) and, in the case of two single sgRNAs, with Cas9 nickase (**Fig. 3a**). High-throughput sequencing to detect indels at the *GFP* target site in cells treated with paired sgRNAs and fCas9, Cas9 nickase, or wild-type Cas9 revealed the expected substantial level of modification ranging from 2.3% to 14.3% of sequence reads. Modification by fCas9 in the presence of any of the four single sgRNAs was not detected above background signal (ranging from <0.01% to 0.073% modification), consistent with the requirement of fCas9 to engage two sgRNAs to cleave DNA. By contrast, Cas9 nickases in the presence of single sgRNAs resulted in modification levels ranging from 0.05% to 0.16% at the target site (**Fig. 3a**). The detection of bona fide indels at target sites following Cas9 nickase treatment with single sgRNAs confirms the mutagenic potential of genomic DNA nicking, consistent with previous reports[3,12,13,16,17]. These results collectively demonstrate that Cas9 nickase can induce genomic DNA modification in the presence of a single sgRNA, in contrast with the absence of single-sgRNA modification by fCas9.

The observed rate of nickase-induced DNA modification did not account for the much higher GFP disruption signal in the flow cytometry assay (**Supplementary Fig. 9b**). Because the sgRNAs that induced GFP signal loss with Cas9 nickase (sgRNAs G1 and G3) both target the nontemplate strand of the GFP gene, and because targeting the nontemplate strand with dCas9 in the coding region of a gene is known to mediate efficient transcriptional repression[24], we speculate that Cas9 nickase combined with the G1 or G3 sgRNAs induced substantial transcriptional repression, in addition to a low level of genome modification. The same effect was not seen for fCas9, suggesting that fCas9 may be more easily displaced from DNA by transcriptional machinery. Taken together, these results indicate that fCas9 can modify genomic DNA efficiently and in a manner that requires simultaneous engagement of two guide RNAs targeting adjacent sites, unlike the ability of wild-type Cas9 and Cas9 nickase to cleave DNA when bound to a sgRNA.

The above results collectively reveal much more stringent spacer, sgRNA orientation, and guide RNA pairing requirements for fCas9 compared with Cas9 nickase. In contrast with fCas9 (**Supplementary Fig. 10**), Cas9 nickase cleaved sites across all spacers assayed (5 to 47 bp in orientation A and 4 to 42 bp in orientation B in this work) (**Fig. 2a,c** and **Supplementary Fig. 8a,b**). These observations are consistent with previous reports of Cas9 nickases modifying sites targeted by sgRNAs with spacer lengths up to 100 bp apart[13,14]. The more stringent spacer and sgRNA orientation requirements of fCas9 compared with Cas9 nickase reduces the number of potential genomic off-target sites of the former by approximately tenfold (**Supplementary Table 1**). Although the more stringent spacer requirements of fCas9 also reduce the number

of potential targetable sites, sequences that conform to the fCas9 spacer and dual PAM requirements exist in the human genome on average once every 34 bp (9.2×10^7 sites in 3.1×10^9 bp) (**Supplementary Table 1**). We also anticipate that the growing number of Cas9 homologs with different PAM specificities[25] will further increase the number of targetable sites using the fCas9 approach.

Improved specificity of fCas9 at endogenous off-target sites

To evaluate the DNA cleavage specificity of fCas9, we measured the modification of known Cas9 off-target sites of *CLTA*, *EMX* and *VEGF* genomic target sites[4,8,9,14]. The target site and its corresponding known off-target sites (**Supplementary Table 2**) were amplified from genomic DNA isolated from HEK293 cells treated with fCas9, Cas9 nickase or wild-type Cas9 and two sgRNAs spaced 19 bp apart targeting the *CLTA* site, two sgRNAs spaced 23 bp apart targeting the *EMX* site, two sgRNAs spaced 14 bp apart targeting the *VEGF* site, or two sgRNAs targeting an unrelated site (GFP) as a negative control. In total 11 off-target sites were analyzed by high-throughput sequencing (**Supplementary Notes**). Sequences containing insertions or deletions of two or more base pairs in potential genomic off-target sites and present in significantly greater numbers ($P < 0.005$, Fisher's exact test) in the target sgRNA-treated samples versus the control sgRNA-treated samples were considered Cas9 nuclease–induced genome modifications. For all 11 off-target sites initially assayed, fCas9 did not result in any detectable genomic off-target modification within the sensitivity limit of our assay (<0.002%, **Supplementary Results**; see further discussion of VEGF off-target site 1 below), while demonstrating substantial on-target modification efficiencies of 5% to 10% (**Fig. 3b–d** and **Supplementary Table 3a–c**). The detailed inspection of fCas9-modified *VEGF* on-target sequences (**Supplementary Fig. 11a**) revealed a prevalence of deletions ranging from two to dozens of base pairs consistent with cleavage occurring in the DNA spacer between the two target binding sites. For each target site at *CLTA*, *EMX* and *VEGF*, fCas9 predominantly induces deletions with insertions representing <5% of all modifications. This prevalence of deletions is also observed with TALENs, which have similar spacer-length preferences[26].

By contrast, genomic off-target DNA cleavage was observed for wild-type Cas9 at all 11 sites assayed. Using the detection limit of the assay as an upper bound for off-target fCas9 activity, we calculated that fCas9 has

a much lower off-target modification rate than wild-type Cas9 nuclease. At the 11 off-target sites modified by wild-type Cas9 nuclease, fCas9 resulted in on-target:off-target modification ratios at least 140-fold higher than that of wild-type Cas9 (**Fig. 3b–d**).

Consistent with previous reports[4,12,14], paired Cas9 nickases also induced substantially fewer off-target modification events (1/11 off-target sites modified at a detectable rate) than wild-type Cas9. An initial high-throughput sequencing assay revealed significant ($P < 10^{-3}$, Fisher's exact test) modification induced by Cas9 nickases in 0.024% of sequences at *VEGF* off-target site 1. This genomic off-target site was not modified by fCas9 despite similar *VEGF* on-target modification efficiencies of 12.3% for Cas9 nickase and 10.4% for fCas9 (**Fig. 3d** and **Supplementary Table 3c**). Because Cas9 nickase-induced modification levels were within an order of magnitude of the limit of detection and fCas9 modification levels were undetected, we repeated the experiment with a larger input DNA samples and a greater number of sequence reads (low input of 150 ng versus high input 600 ng genomic DNA and $>8 \times 10^5$ versus $>23 \times 10^5$ reads for the initial and second trial, respectively) to detect off-target cleavage at this site by Cas9 nickase or fCas9 (**Supplementary Notes**). From this deeper interrogation, we observed Cas9 nickase and fCas9 to both significantly modify ($P < 10^{-5}$, Fisher's exact test) *VEGF* off-target site 1 (**Fig. 3e**, **Supplementary Table 3d** and **Supplementary Fig. 11b**). For both experiments interrogating the modification rates at *VEGF* off-target site 1, fCas9 exhibited a greater on-target/off-target DNA modification ratio than that of Cas9 nickase (>5,150 and 1,650 for fCas9, versus 510 and 1,230 for Cas9 nickase, **Fig. 3e**).

To further investigate differences in specificity between fCas9 and Cas9 nickases, three new target sites (sites A, B, and C) were chosen in the human genome that each had potential genomic off-target sites containing one identical or nearly identical half-site (**Supplementary Table 4**). The three on-target sites and their highly similar off-target sites were amplified and sequenced from cells treated with a mock transfection of a GFP expression plasmid, fCas9, or Cas9 nickases and either two sgRNAs spaced 15 bp apart targeting genomic site A, two sgRNA spaced 24 bp apart targeting genomic site B, or two sgRNA spaced 23 bp apart targeting genomic site C. At these three sites fCas9 demonstrated greater than fourfold average increase in on-target/off-target genome modification activity compared to Cas9 nickases (**Fig. 4** and **Supplementary Table 5**). These results suggest that for highly similar sets of on- and off-target sites, as may be found with repetitive genomic loci, pseudogenes or homologous gene families, fCas9 can result in improved genome modification specificity over that of Cas9 nickases.

DISCUSSION

In this work, we developed fCas9, an obligate dimeric FokI-dCas9 nuclease architecture. The fCas9 nuclease modified all 11 genomic loci tested with sgRNA pairs spaced ~15 bp or ~25 bp apart, demonstrating the generality of using fCas9 to induce genomic modification in human cells. The use of fCas9 is straightforward, requiring only that PAM sequences be present with an appropriate spacing and orientation, and using the same sgRNA architecture as wild-type Cas9 or Cas9 nickases.

Although modification with fCas9 was generally less efficient than with wild-type Cas9, fCas9 was consistently more specific, producing substantially fewer off-target modification
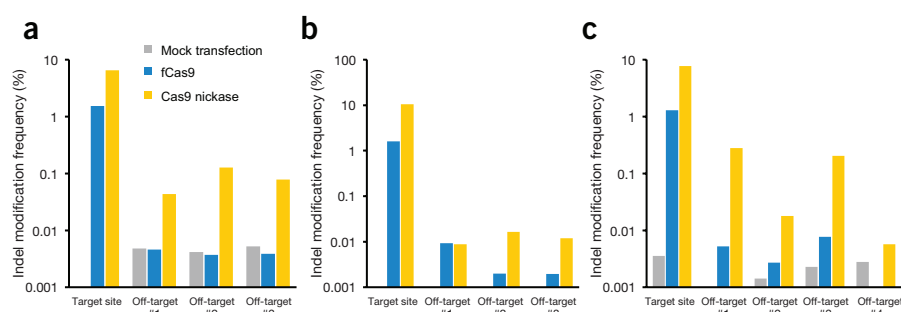

Figure 4 Genomic DNA modification specificity of fCas9 and Cas9 nickase at genomic sites with highly similar off-target sites. (**a**–**c**) The indel mutation frequency from high-throughput DNA sequencing of amplified genomic on-target sites and off-target sites (**Supplementary Table 4**) from human cells treated with fCas9 or Cas9 nickase and two sgRNAs (sgRNAs SA1 and SA2) spaced 15 bp apart targeting site A, human genomic locus chr1:21,655,401-21,655,461 (**a**); two sgRNAs (sgRNAs SB1 and SB2) spaced 24 bp apart targeting site B, human genomic locus chr2:31,485,447-31,485,516 (**b**); or two sgRNAs (sgRNAs SC1 and SC2) spaced 23 bp apart targeting the site C, human genomic locus chr3:48,747,484-48,747,552 (**c**). *P* values are listed in **Supplementary Table 5**. Each on- and off-target sample was sequenced once with >10,000 sequences analyzed per on-target sample and an average of 83,000 sequences analyzed per off-target sample (**Supplementary Table 5**). The mock transfection control represents the limit of detection for each site, determined from cells transfected with a GFP expression plasmid and no sgRNA or nuclease expression constructs.

events. The observed low off-target/on-target modification ratios of fCas9 were at least 140-fold lower than that of wild-type Cas9 and from 1.3- to 8.8-fold lower than that of paired Cas9 nickases. These improvements likely arise from the distinct mode of action of dimeric FokI, which cleaves DNA only if two sites are occupied simultaneously by two FokI domains at a specified distance (here, ~15 bp or ~25 bp apart) and in a specific half-site orientation. Indeed, when presented with only a single sgRNA (**Fig. 3a**), or a single matching half-site at off-target genomic loci (**Fig. 4**), fCas9 was unable to modify DNA. Given our use of plasmid transfection in this study, more efficient gene delivery methods such as nucleofection may offer higher fCas9 modification efficiency.

The only observed off-target DNA modification by fCas9 in this study was the modification of the *VEGF* off-target site 1. On either side of the *VEGF* off-target site 1, there exist no other sites with six or fewer mutations from either of the two half-sites of the *VEGF* on-target sequence. We speculate that the first 11 bases of one sgRNA (V2) might hybridize to the single-stranded DNA freed by canonical Cas9:sgRNA binding within VEGF off-target site 1 (**Supplementary Fig. 11c**). Through this sgRNA:DNA hybridization it is possible that a second Cas9 nickase or fCas9 could be recruited to modify this off-target site at an extremely rare, but detectable frequency.

A recent report[27] demonstrates the promiscuity of dCas9 binding to sequences containing only an NGG PAM and a "seed" sequence as short at five bases immediately 5′ of the PAM. A search of the sequence surrounding VEGF off-target site 1 identified a single site of this type, with a single mismatch within the six bases 5′ of an NGG PAM (**Supplementary Fig. 11d**). This potential site corresponds to an untested sgRNA pair orientation, and is likely a very inefficient substrate for fCas9 cleavage. Judicious sgRNA pair design could eliminate either of these potential modes of off-target DNA cleavage at sites similar to *VEGF* off-target site 1. The promiscuity of dCas9 binding at short seed-PAM sequences may be mitigated by the requirement of fCas9 to assemble on two dCas9 binding sites with very specific spacer constraints and PAM orientations.

The low off-target activity of fCas9 may enable applications of Cas9:sgRNA-based technologies that require a very high degree of target specificity, such as *ex vivo* or *in vivo* therapeutic modification of human cells. This work also provides a foundation for future studies to characterize in greater detail and further improve the DNA cleavage activity and specificity of fCas9 *in vitro* and *in vivo*. For example, the use of recently described orthogonal Cas9 homologs[25] coupled with obligate heterodimeric FokI variants[28] may offer additional specificity gains.

METHODS

Methods and any associated references are available in the online version of the paper.

Accession codes. SRA: SRP041161.

Note: Any Supplementary Information and Source Data files are available in the online version of the paper.

AUTHOR CONTRIBUTIONS
J.P.G. and D.B.T. performed the experiments, designed the research, analyzed the data and wrote the manuscript. D.R.L. designed the research, analyzed the data and wrote the manuscript.

COMPETING FINANCIAL INTERESTS
The authors declare competing financial interests: details are available in the online version of the paper.

Reprints and permissions information is available online at http://www.nature.com/reprints/index.html.

1. Shalem, O. *et al.* Genome-scale CRISPR-Cas9 knockout screening in human cells. *Science* **343**, 84–87 (2014).
2. Perez, E.E. *et al.* Establishment of HIV-1 resistance in CD4+ T cells by genome editing using zinc-finger nucleases. *Nat. Biotechnol.* **26**, 808–816 (2008).
3. Mali, P. *et al.* RNA-guided human genome engineering via Cas9. *Science* **339**, 823–826 (2013).
4. Fu, Y., Sander, J.D., Reyon, D., Cascio, V.M. & Joung, J.K. Improving CRISPR-Cas nuclease specificity using truncated guide RNAs. *Nat. Biotechnol.* **32**, 279–284 (2014).
5. Jinek, M. *et al.* A programmable dual-RNA-guided DNA endonuclease in adaptive bacterial immunity. *Science* **337**, 816–821 (2012).
6. Cong, L. *et al.* Multiplex genome engineering using CRISPR/Cas systems. *Science* **339**, 819–823 (2013).
7. Jinek, M. *et al.* RNA-programmed genome editing in human cells. *eLife* **2**, e00471 (2013).
8. Pattanayak, V. *et al.* High-throughput profiling of off-target DNA cleavage reveals RNA-programmed Cas9 nuclease specificity. *Nat. Biotechnol.* **31**, 839–843 (2013).
9. Fu, Y. *et al.* High-frequency off-target mutagenesis induced by CRISPR-Cas nucleases in human cells. *Nat. Biotechnol.* **31**, 822–826 (2013).
10. Hsu, P.D. *et al.* DNA targeting specificity of RNA-guided Cas9 nucleases. *Nat. Biotechnol.* **31**, 827–832 (2013).
11. Cradick, T.J., Fine, E.J., Antico, C.J. & Bao, G. CRISPR/Cas9 systems targeting β-globin and CCR5 genes have substantial off-target activity. *Nucleic Acids Res.* **41**, 9584–9592 (2013).
12. Cho, S.W. *et al.* Analysis of off-target effects of CRISPR/Cas-derived RNA-guided endonucleases and nickases. *Genome Res.* **24**, 132–141 (2014).
13. Mali, P. *et al.* CAS9 transcriptional activators for target specificity screening and paired nickases for cooperative genome engineering. *Nat. Biotechnol.* **31**, 833–838 (2013).
14. Ran, F.A. *et al.* Double nicking by RNA-guided CRISPR Cas9 for enhanced genome editing specificity. *Cell* **154**, 1380–1389 (2013).
15. Gasiunas, G., Barrangou, R., Horvath, P. & Siksnys, V. Cas9-crRNA ribonucleoprotein complex mediates specific DNA cleavage for adaptive immunity in bacteria. *Proc. Natl. Acad. Sci. USA* **109**, E2579–E2586 (2012).
16. Ramirez, C.L. *et al.* Engineered zinc finger nickases induce homology-directed repair with reduced mutagenic effects. *Nucleic Acids Res.* **40**, 5560–5568 (2012).
17. Wang, J. *et al.* Targeted gene addition to a predetermined site in the human genome using a ZFN-based nicking enzyme. *Genome Res.* **22**, 1316–1326 (2012).
18. Vanamee, É.S., Santagata, S. & Aggarwal, A.K. FokI requires two specific DNA sites for cleavage. *J. Mol. Biol.* **309**, 69–78 (2001).
19. Pattanayak, V., Ramirez, C.L., Joung, J.K. & Liu, D.R. Revealing off-target cleavage specificities of zinc-finger nucleases by *in vitro* selection. *Nat. Methods* **8**, 765–770 (2011).
20. Guilinger, J.P. *et al.* Broad specificity profiling of TALENs results in engineered nucleases with improved DNA-cleavage specificity. *Nat. Methods* **11**, 429–435 (2014).
21. Nishimasu, H. *et al.* Crystal structure of Cas9 in complex with guide RNA and target DNA. *Cell* **156**, 935–949 (2014).
22. Jinek, M. *et al.* Structures of Cas9 endonucleases reveal RNA-mediated conformational activation. *Science* **31**, 6176 (2014).
23. Schellenberger, V. *et al.* A recombinant polypeptide extends the *in vivo* half-life of peptides and proteins in a tunable manner. *Nat. Biotechnol.* **27**, 1186–1190 (2009).
24. Qi, L.S. *et al.* Repurposing CRISPR as an RNA-guided platform for sequence-specific control of gene expression. *Cell* **152**, 1173–1183 (2013).
25. Esvelt, K.M. *et al.* Orthogonal Cas9 proteins for RNA-guided gene regulation and editing. *Nat. Methods* **10**, 1116–1121 (2013).
26. Kim, Y., Kweon, J. & Kim, J.-S. TALENs and ZFNs are associated with different mutation signatures. *Nat. Methods* **10**, 185–185 (2013).
27. Wu, X. *et al.* Genome-wide binding of the CRISPR endonuclease Cas9 in mammalian cells. *Nat. Biotechnol.* doi:10.1038/nbt.2889 (20 April 2014).
28. Doyon, Y. *et al.* Enhancing zinc-finger-nuclease activity with improved obligate heterodimeric architectures. *Nat. Methods* **8**, 74–79 (2011).

ONLINE METHODS

Oligonucleotides and PCR. All oligonucleotides were purchased from Integrated DNA Technologies (IDT). Oligonucleotide sequences are listed in **Supplementary Notes**. PCR was performed with 0.4 μl of 2 U/μl Phusion Hot Start Flex DNA polymerase (NEB) in 50 μl with 1× HF Buffer, 0.2 mM dNTP mix (0.2 mM dATP, 0.2 mM dCTP, 0.2 mM dGTP, 0.2 mM dTTP) (NEB), 0.5 μM of each primer and a program of: 98 °C, 1 min; 35 cycles of (98 °C, 15 s; 65 °C, 15 s; 72 °C, 30 s) unless otherwise noted.

Construction of FokI-dCas9, Cas9 nickase and sgRNA expression plasmids. The human codon-optimized *Streptococcus pyogenes* Cas9 nuclease with NLS and 3×FLAG tag (Addgene plasmid 43861)[9] was used as the wild-type Cas9 expression plasmid. PCR (72 °C, 3 min) products of wild-type Cas9 expression plasmid as template with Cas9_Exp primers listed in **Supplementary Notes** were assembled with Gibson Assembly Cloning Kit (New England Biolabs) to construct Cas9 and FokI-dCas9 variants. Expression plasmids encoding a single sgRNA construct (sgRNA G1 through G13) were cloned as previously described[9]. Briefly, sgRNA oligonucleotides listed in **Supplementary Notes** containing the 20-bp protospacer target sequence were annealed and the resulting 4-bp overhangs were ligated into BsmBI-digested sgRNA expression plasmid. sgRNA expression plasmids encoding expression of two separate sgRNA constructs from separate promoters on a single plasmid were cloned in a two-step process depicted in **Supplementary Notes**. First, one sgRNA (sgRNA E1, V1, C1, C3, H1, G1, G2 or G3) was cloned as above and used as a template for PCR (72 °C, 3 min) with PCR_Pla-fwd and PCR_Pla-rev primers, 1 μl DpnI (NEB) was added, and the reaction was incubated at 37 °C for 30 min and then subjected to QIAquick PCR Purification Kit (Qiagen) for the "1st sgRNA + vector DNA." PCR (72 °C, 3 min) of 100 pg of BsmBI-digested sgRNA expression plasmid as template with PCR_sgRNA-fwd1, PCR_sgRNA-rev1, PCR_sgRNA-rev2 and appropriate PCR_sgRNA primer listed in **Supplementary Notes** was DpnI treated and purified as above for the "2nd sgRNA insert DNA." ~200 ng of "1st sgRNA + vector DNA" and ~200 ng of "2nd sgRNA insert DNA" were blunt-end ligated in 1 × T4 DNA Ligase Buffer, 1 μl of T4 DNA Ligase (400 U/μl, NEB) in a total volume of 20 μl at room temperature (~21 °C) for 15 min. For all cloning, 1 μl of ligation or assembly reaction was transformed into Mach1 chemically competent cells (Life Technologies). Protein and DNA sequences are listed in **Supplementary Notes**. The optimized FokI-dCas9 (fCas9) expression plasmid is available from Addgene (52970).

Modification of genomic GFP. HEK293-GFP stable cells (GenTarget) were used as a cell line constitutively expressing an Emerald GFP gene (*GFP*) integrated on the genome. Cells were maintained in Dulbecco's modified Eagle medium (DMEM, Life Technologies) supplemented with 10% (vol/vol) FBS (FBS, Life Technologies) and penicillin/streptomycin (1×, Amresco). $5 × 10^4$ HEK293-GFP cells were plated on 48-well collagen-coated Biocoat plates (Becton Dickinson). One day after plating, cells at ~75% confluence were transfected with Lipofectamine 2000 (Life Technologies) according to the manufacturer's protocol. Briefly, 1.5 μl of Lipofectamine 2000 was used to transfect 950 ng of total plasmid (Cas9 expression plasmid plus sgRNA expression plasmids). 700 ng of Cas9 expression plasmid, 125 ng of one sgRNA expression plasmid and 125 ng of the paired sgRNA expression plasmid with the pairs of targeted sgRNAs listed in **Figure 1d** and **Supplementary Figure 1a**. Separate wells were transfected with 1 μg of a near-infrared iRFP670 (Addgene plasmid 45457)[29] as a transfection control. Transfection efficiencies ranged from 70% to 80% per construct. 3.5 d after transfection, cells were trypsinized and resuspended in DMEM supplemented with 10% FBS and analyzed on a C6 flow cytometer (Accuri) with a 488-nm laser excitation and 520-nm filter with a 20-nm band pass. For each sample, transfections and flow cytometry measurements were performed once.

T7 endonuclease I surveyor assays of genomic modifications. HEK293-GFP stable cells were transfected with Cas9 expression and sgRNA expression plasmids as described above. A single plasmid encoding two separate sgRNAs was transfected. For experiments titrating the total amount of expression plasmids (Cas9

expression + sgRNA expression plasmid), 700/250, 350/125, 175/62.5, 88/31 ng of Cas9 expression plasmid/ng of sgRNA expression plasmid were combined with inert carrier plasmid, pUC19 (NEB), as necessary to reach a total of 950 ng transfected plasmid DNA.

Genomic DNA was isolated from cells 2 d after transfection using a genomic DNA isolation kit, DNAdvance Kit (Agencourt). Briefly, cells in a 48-well plate were incubated with 40 μl of trypsin for 5 min at 37 °C. 160 μl of DNAdvance lysis solution was added and the solution incubated for 2 h at 55 °C and the subsequent steps in the Agencourt DNAdvance kit protocol were followed. 40 ng of isolated genomic DNA was used as template to PCR amplify the targeted genomic loci with flanking Survey primer pairs specified in the **Supplementary Notes**. PCR products were purified with a QIAquick PCR Purification Kit (Qiagen) and quantified with Quant-iT PicoGreen dsDNA Kit (Life Technologies). 250 ng of purified PCR DNA was combined with 2 μl of NEBuffer 2 (NEB) in a total volume of 19 μl and denatured then re-annealed with thermocycling at 95 °C for 5 min, 95–85 °C at 2 °C/s; 85–20 °C at 0.2 °C/s. The re-annealed DNA was incubated with 1 μl of T7 Endonuclease I (10 U/μl, NEB) at 37 °C for 15 min. 10 μl of 50% glycerol was added to the T7 Endonuclease reaction and 12 μl was analyzed on a 5% TBE 18-well Criterion PAGE gel (Bio-Rad) electrophoresed for 30 min at 150 V, then stained with 1× SYBR Gold (Life Technologies) for 30 min. Cas9-induced cleavage bands and the uncleaved band were visualized on an AlphaImager HP (Alpha Innotech) and quantified using ImageJ software[30]. The peak intensities of the cleaved bands were divided by the total intensity of all bands (uncleaved + cleaved bands) to determine the fraction cleaved, which was used to estimate gene modification levels as previously described[31]. For each sample, transfections and subsequent modification measurements were performed in triplicate on different days.

High-throughput sequencing of genomic modifications. HEK293-GFP stable cells were transfected with plasmids expressing Cas9 and sgRNAs. Generally, 700 ng of Cas9 expression plasmid (encoding either fCas9, Cas9 nickase or Cas9 nuclease) plus 250 ng of a single plasmid expressing a pair of sgRNAs were transfected. (See **Supplementary Fig. 7** and **Supplementary Table 3** for additional details.) Genomic DNA was isolated as above and pooled from three biological replicates. 150 ng or 600 ng of pooled genomic DNA was used as template to amplify by PCR the on-target and off-target genomic sites with flanking HTS primer pairs specified in the **Supplementary Notes**. Relative amounts of crude PCR products were quantified by gel electrophoresis, and samples treated with different sgRNA pairs or Cas9 nuclease types were separately pooled in equimolar concentrations before purification with the QIAquick PCR Purification Kit (Qiagen). ~500 ng of pooled DNA was run on a 5% TBE 18-well Criterion PAGE gel (Bio-Rad) for 30 min at 200 V, and DNAs of length ~125 bp to ~300 bp were isolated and purified by QIAquick PCR Purification Kit (Qiagen). Purified DNA was PCR amplified with primers containing sequencing adaptors, purified and sequenced on a MiSeq high-throughput DNA sequencer (Illumina) as described previously[8].

Data analysis. Illumina sequencing reads were filtered and parsed with scripts written in Unix Bash as outlined in **Supplementary Notes**. The source code was published previously[20]. DNA sequences will be deposited in NCBI's Sequencing Reads Archive (SRA). Sample sizes for sequencing experiments were maximized (within practical experimental considerations) to ensure the greatest power to detect effects. Statistical analyses for Cas9-modified genomic sites in **Supplementary Table 3** were performed as previously described[32] with multiple comparison correction using the Bonferroni method.

29. Shcherbakova, D.M. & Verkhusha, V.V. Near-infrared fluorescent proteins for multicolor *in vivo* imaging. *Nat. Methods* **10**, 751–754 (2013).
30. Schneider, C.A., Rasband, W.S. & Eliceiri, K.W. NIH Image to ImageJ: 25 years of image analysis. *Nat. Methods* **9**, 671–675 (2012).
31. Guschin, D.Y. *et al.* in *Engineering Zinc Finger Proteins* (eds. Mackay, J.P. & Segal, D.J.) 247–256 (Humana Press, 2010).
32. Sander, J.D. *et al. In silico* abstraction of zinc finger nuclease cleavage profiles reveals an expanded landscape of off-target sites. *Nucleic Acids Res.* **41**, e181 (2013).